

Measurements of kinematical parameters of spiral waves in media of low excitability

On-Uma Kheowan,^{†a} Vilmos Gáspár,^{*b} Vladimir S. Zykov^a and Stefan C. Müller^a

^a Institut für Experimentelle Physik, Otto-von-Guericke-Universität, Universitätsplatz 2, D-39106, Magdeburg, Germany

^b Institute of Physical Chemistry, University of Debrecen, H-4010 Debrecen, P.O. Box 7, Hungary. E-mail: gasparv@delfin.klte.hu

Received 21st May 2001, Accepted 28th August 2001

First published as an Advance Article on the web 11th October 2001

The dynamics of spiral waves rotating in a thin layer of the light sensitive Belousov–Zhabotinsky reaction mixture are studied under a homogeneous and steady illumination. At a given composition of the excitable medium, the spiral waves meand, when no or low intensity light is applied, or rigidly rotate, when the light intensity is increased sufficiently. There exists, however, a critical value of light intensity above which no wave activity is supported by the medium, since its excitability is too strongly reduced by the illumination. In the vicinity of this critical value the basic kinematical parameters of rigidly rotating spirals (such as the rotation period, wavelength, propagation velocity, and the diameter of the spiral core) are measured as a function of the illumination intensity. The experimental observations are in good agreement with the predictions based on an earlier proposed kinematical theory of spiral waves in media of low excitability.

Introduction

Spiral waves have been observed in a variety of excitable media such as cardiac muscle tissue,¹ CO oxidation on platinum surfaces² and the Belousov–Zhabotinsky (BZ) reacting mixture.^{3–5} Among these systems, the BZ reaction is the most suitable laboratory system to study the dynamics of these waves, especially when the light sensitive Ru(bpy)₃²⁺ catalyst is applied. Here the excitability of the medium (and thus the dynamics of waves) can be easily controlled by varying the illumination intensity.^{6–13}

It has been shown, for example, that at a given composition of the BZ reaction the trajectory of the spiral tip depends strongly on the illumination intensity.¹⁰ Moreover, illumination of sufficiently high intensity can even suppress any wave activity in the medium. In the vicinity of this critical intensity level, spiral waves are found to rotate rigidly around a circular core.¹³

The rigid rotation of a spiral wave in an excitable medium can be characterized by well-defined kinematical parameters such as the rotation period, wavelength, propagation velocity, and the diameter of the spiral core. The properties of this dynamical regime have been studied experimentally^{4,5} and analyzed theoretically.^{4,14–16} In particular, it was found that for the case of low excitability certain relations between different kinematical parameters of the rigidly rotating spiral waves should exist.¹⁵

In this paper, we report on the experimental determination of the kinematical parameters of rigidly rotating spirals as a function of the illumination intensity allowing, for the first time, a direct test of the theoretical predictions.

Experimental method

The experimental set-up is that applied in our previous studies.^{11–13} In order to minimize 3D effects, a very thin

(0.33 ± 0.02 mm) layer of silica gel (2 ml of a mixture of 2 ml 15% water glass, 0.612 ml 0.0206 M Ru(bpy)₃SO₄, 0.092 ml 5 M H₂SO₄ and 0.296 ml H₂O) is prepared in a petri dish of 7 cm diameter. The thickness of the layer is always measured by a microscrewmeter. The light sensitive Ru(bpy)₃²⁺ catalyst is immobilized in the gel as described earlier.¹⁷ Its concentration in the gel was kept constant at 4.2 mM.

In all experiments, 2 ml BZ mixture without catalyst (composed of 1.00 ml 1 M NaBrO₃, 0.21 ml 4 M MA, 0.45 ml H₂O, 0.39 ml 5 M H₂SO₄ and 0.45 ml 1 M NaBr) is placed on the top of the gel. When the phase equilibrium between the liquid and gel has been practically established (after a few minutes), the following concentrations are reached: [NaBrO₃]: 0.2 M, [malonic acid]: 0.17 M, [H₂SO₄]: 0.39 M, and [NaBr]: 0.09 M. (Note that the slow bromination of malonic acid was neglected.) In addition, the reservoir can be enlarged by adding a volume of typically 8 ml of BZ mixture diluted to half the concentration values specified above. The gel and the solution were kept at an ambient temperature of 22 ± 1 °C.

The gel in the petri dish is uniformly illuminated from below with a video projector (Panasonic PT-L555E) controlled by a computer *via* a frame grabber (Data Translation, DT 2851). The light of the video projector is filtered with a band-pass filter (BG6, 310–530 nm). The intensity of the light passed through the filter was measured before each experiment by using a photometer (Tektronix, J 1812). The photometer was put in exactly the position of the Petri dish during the experiments.

The oxidation waves are observed in transmitted light by a CCD camera (Hamamatsu H 3077) from above the gel, due to the difference between the absorption of the oxidized and the reduced state of the catalyst. To further enhance the images a narrow band pass filter (490 nm) is placed between the gel and the camera. The images were stored on a video recorder (Sony EVT 301).

At the beginning of an experiment the oxidation waves begin to emerge spontaneously, usually at the boundary of the

[†] Permanent address: Department of Chemistry, Mahidol University, Rama 6 Road, Bangkok 10400, Thailand.

petri dish. A cold light source of high illumination intensity (Schott, KL 1500) is applied to break a spontaneously formed wavefront in the middle of the dish, where it has a practically planar shape. The light source provides a circular spot (diameter, 1 cm) of local illumination of the gel. Since inside this spot the wave activity is completely suppressed, the front of a travelling wave is broken and two open ends are formed that evolve into a pair of counter-rotating spirals. Subsequently, the light spot is applied to the open end of one of the spirals and slowly shifted along its wavefront towards the boundary of the dish. This procedure allows one to erase the spiral as one removes a pen trace with an eraser. The other single spiral remaining in the center of the dish constitutes the initial condition for all reported experiments.

In order to characterize the main features of spiral rotation, it suffices to consider the trajectory of the spiral tip. The location of a given spiral tip is determined by the following procedure. Contour lines ($0.6 \times$ wave amplitude) of spiral images are extracted from two consecutive frames of the digitized movie with a time step of 3.12 s. The tip is defined as the intersection point of these two contour lines. The location of this point in the frame is determined by a special computer procedure.¹⁸ The trajectory of the tip is obtained by connecting the temporal sequence of the points representing the location of the tip for each time step.

Experimental observations

Fig. 1 shows snapshots of rotating waves at two different light intensities, $I = 1.8$ and 2.0 W m^{-2} , respectively. In Fig. 1(a), the tip rotates rigidly around a closed circle that marks the boundary of the spiral core. On the other hand, when switching to a higher intensity ($I = 2.0 \text{ W m}^{-2}$), the tip of the spiral wave moves away from the center of the observation area due to a pronounced increase in the core radius, as indicated by the trajectory in Fig. 1(b). The travelling of the spiral tip

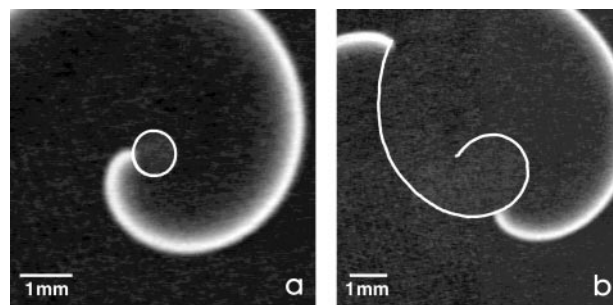


Fig. 1 Rigid rotation (a) and disappearance (b) of a spiral wave from the observation area. Curves show the trajectories of the spiral tip at $I = 1.8 \text{ W m}^{-2}$ (a) and $I = 2.0 \text{ W m}^{-2}$ (b). In image (b) two snapshots of the spiral are shown at $t = 164$ and 421 s after the intensity was switched from 1.8 to 2.0 W m^{-2} .

during this experiment is shown by its trajectory overlaid on the spiral images taken at $t = 164$ and 421 s , respectively. One can foresee that the tip will soon disappear from the observation area.

A systematic study of the influence of the illumination intensity on the tip movement has been determined in a series of experiments. The trajectories of the spiral tip shown in Fig. 2(a) illustrate that at rather low light intensities ($0.2\text{--}0.6 \text{ W m}^{-2}$) the spiral tip moves on a hypocycloid composed of four loops. The dynamics of these loops has been discussed in detail earlier.^{5,19}

Interestingly, under rather strong illumination (0.8 W m^{-2} and higher), the spiral wave rotates rigidly and the wave tip moves on a closed circle comprising a spiral core. The core radius of these rigidly rotating spirals increases with increasing illumination intensity. It can be clearly seen, that there exists a critical value of the light intensity, above which the spiral tip travels all the way to the boundary of the gel

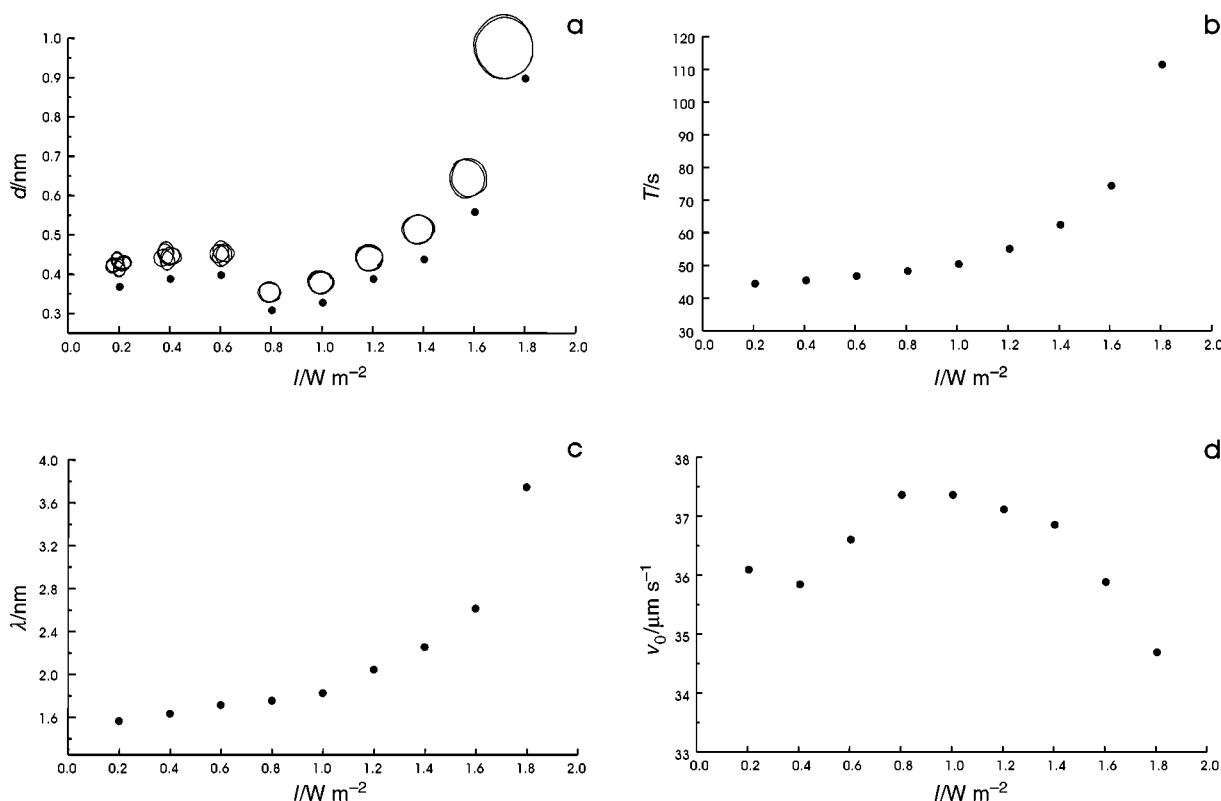


Fig. 2 Experimentally determined kinematical parameters as a function of the light intensity, I : (a) diameter of spiral core, d , with overlaid spiral tip trajectories (10 times enlarged), (b) rotation period, T , and (c) wavelength, λ , of spirals and (d) propagation velocity, v_0 , of a propagating wave far away from the spiral core.

medium, which in turn will lead to the disappearance of the spiral wave itself (*cf.* Fig. 1(b)). That is, the spiral wave propagation in the excitable medium is completely suppressed at these high intensities.

In order to quantify these observations the kinematical parameters of the rigidly rotating spirals were determined as follows. The diameter of the spiral core, d , is calculated as the average diameter of the circular trajectories of the spiral tip. The rotation period, T , is determined as the average time during which two consecutive wavefronts reach a predefined measuring point. The wavelength, λ , is computed as the average length of the normal vector connecting two consecutive wavefronts. The propagation velocity, v_0 , was derived from the time–space plot of a propagating wave. Parameters T , λ and v_0 were determined from data measured relatively far away (at a distance of at least 2–3 λ) from the center of rotation, where the curvature of the front is very small.

Obviously, the variation in the light intensity affects all of the characteristics of a rotating spiral. The solid dots in Fig. 2(a) indicate a significant growth of the core diameter as the light intensity is increased from 0.6 to 1.8 W m^{-2} . The experimentally determined values of T , λ and v_0 are plotted as a function of the light intensity in Fig. 2(b), (c) and (d), respectively. Both T and λ increase to infinity as the light intensity is increased, which is similar to the finding for the core size d (Fig. 2(a)). Note that v_0 varies only within a small range ($\pm 5\%$) around an average value.

Kinematical consideration

In order to interpret the obtained dependences of the measured parameters on the illumination intensity, let us consider the kinematics of a rotating spiral wave. A scheme of a rigidly rotating spiral wave is shown in Fig. 3. Points q and Q on the contour line of the excitation wave correspond to the shortest and the tangential radius-vectors, r_q and r_Q , respectively. Each point of the contour line is involved in a visible rotatory motion that occurs at the speed $u = \omega r$, where ω is the rotation frequency and r is the distance from the rotation center. On the other hand, the real displacement of the wave front occurs in the normal direction with respect to the contour line due to the physical nature of the travelling excitation waves.

Point q does not move in the normal direction. Its location can be determined as the intersection of contour lines plotted at two close instants (see Experimental method). This corresponds to the definition of the spiral tip used in our experiments. Indeed, the circle in Fig. 3 is the trajectory of the spiral wave tip determined as the intersection of contour lines plotted at two close instants separated by time step $\Delta t = 3.12$ s. In the theoretical limit $\Delta t \rightarrow 0$ the spiral wave tip should coincide with point q .

Point Q also plays an important role in the kinematical description of the spiral wave, because its visible rotation

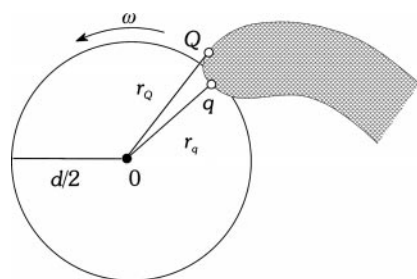


Fig. 3 Scheme of the rotating spiral wave, where d is the diameter of the spiral core and ω is the rotation frequency of the spiral tip. The circular path shows the trajectory of the spiral tip. Points q and Q on the contour line of the excitation wave (shaded area) correspond to the shortest and the tangential radius-vectors, r_q and r_Q , respectively.

around the center coincides with the displacement in the normal direction to the wave front. The trajectory of the point Q can be considered as the boundary of a circular hole around which the spiral wave circulates. Under the assumption of a constant normal propagation velocity $v = v_0$, it was shown that the shape of the spiral around such a hole represents the involute of the hole.^{4,20} This geometrical consideration agrees well with findings from experiments in nonhomogeneous media.^{21,22}

In our experiments we are dealing with a spiral that rotates freely in a homogeneous medium. The size of the spiral wave core in this case is a natural feature of the medium, rather than the diameter of an artificially made hole. However, the shape of the rotating spiral is very similar to the involute of the circular trajectory of the point Q , and some basic relationships between the spiral wave parameters are valid and useful. For example, in the framework of the Wiener model,²⁰ the rotation period of a spiral wave circulating around a hole is a linear function of the diameter d :

$$T = \pi d/v_0 \quad (1)$$

and the wavelength λ of the spiral should also be proportional to the diameter d :

$$\lambda = \pi d. \quad (2)$$

These predictions agree rather well with the dependences shown in Fig. 4, where the mutual relationships between the measured kinematical characteristics are presented. Indeed, the period, T (left axis), and the wavelength, λ (right axis), are practically linear functions of d . The experimental data can be well approximated by using the following equations (calculated with linear regression): $T/\text{s} = 15.12 + 107.5d/\text{mm}$ and $\lambda/\text{mm} = 0.74 + 3.35d/\text{mm}$. Note that the intercepts are not equal to zero for both functions. The reason for this discrepancy is that the measured value d is not the diameter of the trajectory of point Q , as is clearly seen in Fig. 3. More precise formulae for $T(d)$ and for $\lambda(d)$ can be written as

$$T = \pi(d + \Delta)/v_0 \quad (3)$$

and

$$\lambda = \pi(d + \Delta)v_0/v_Q, \quad (4)$$

where Δ is the difference between the diameters of the trajectories of points Q and q , and v_Q is the normal propagation velocity at point Q . The calculated intercept for $\lambda(d)$ allows one to estimate the difference $\Delta = 0.22$ mm corresponding to our experiments. It is not surprising that this value is relatively small, because in media of low excitability the wave is rather thin with respect to the core size and, therefore, points q and Q are close to each other.

A more elaborate kinematical description of a freely rotating spiral in a medium of low excitability is based on the assumption that the normal propagation velocity, v , of a

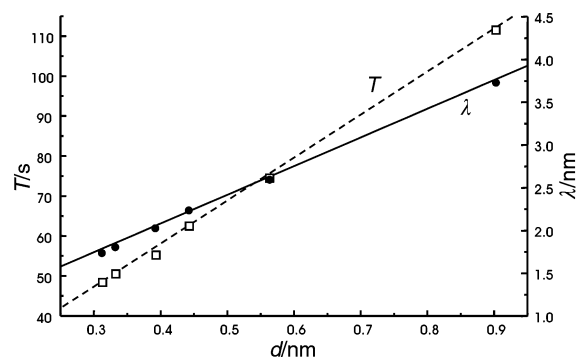


Fig. 4 Mutual relations between the kinematical parameters: rotation period, T , and wavelength, λ , as a function of the core diameter, d .

curved wavefront is a linear function of its curvature, κ .¹⁵ If the curvature is considered positive for a convex wavefront, the so-called eikonal equation is written as

$$v(\kappa) = v_0 - D\kappa, \quad (5)$$

where v_0 is the velocity of a plane wave and D is the diffusion coefficient of the activator species in the medium.

Far away from point Q the curvature of the wavefront vanishes and the propagation velocity is practically constant: $v = v_0$. However, the curvature at point Q , κ_Q , is positive and $v_Q < v_0$. Due to this, the shape of a freely rotating spiral differs from the involute of the trajectory of point Q .

In order to determine this shape, it is useful to specify the curvature κ as a function of the arc length s : $\kappa = \kappa(s)$ (the natural equation of a curve). All the points of a spiral wavefront move in the normal direction with velocity $v(\kappa)$, which results in a variation of the local curvature. On the other hand, the resulting displacement of the front as a whole looks like the rotation of the spiral without any change in its shape. In order to fulfill these conditions, the function $\kappa(s)$ should obey the following integrodifferential equation¹⁵

$$D \frac{d\kappa}{ds} = \kappa \int_0^s \kappa v ds' - \omega \quad (6)$$

with two boundary conditions

$$\kappa(0) = \kappa_Q; \quad \kappa(\infty) = 0. \quad (7)$$

Here $\omega = 2\pi/T$ is the rotation frequency. The value of ω can be obtained as a solution to the nonlinear boundary problem (eqn. (6) and (7)). Obviously, the value of the rotation frequency, ω , should be a function of the parameters in the eikonal equation: v_0 , D and κ_Q . Taking into account the dimensions of these parameters, the rotation frequency can be expressed as¹⁵

$$\omega = v_0 \kappa_Q \varphi(\eta) = \frac{v_0^2 \eta \varphi(\eta)}{D}, \quad (8)$$

where $\psi(\eta)$ is a well defined function of the dimensionless curvature, η

$$\eta = \frac{D\kappa_Q}{v_0}. \quad (9)$$

The exact functional form $\psi(\eta)$ is not known. However, the numerically determined values can be well approximated by the following expression¹⁵

$$\varphi(\eta) = 0.685\eta^{1/2} - 0.06\eta - 0.293\eta^2. \quad (10)$$

An important limiting case is $\eta = 1$ which corresponds to the maximal possible curvature at the point Q : $\kappa_Q = v_0/D$. According to eqn. (10), $\psi(1) = 0.33$. We note that the same value has been found earlier in numerical solutions to the problem of crystal growth.¹⁴ The other limiting case is $\eta \ll 1$ corresponding to a very small curvature κ_Q . In this case the shape of the wavefront has been found analytically, and an expression for the rotation frequency has been obtained that coincides with the first term of eqn. (10).²³

According to eqn. (8), the dimensionless parameter η plays an important role in determining the frequency of spiral rotation. Experimental values for D and v_0 are readily available but, unfortunately, it is quite difficult to determine the value of κ_Q from the contour lines of spiral waves detected with a CCD camera. Therefore, one has to find an indirect way to determine the value of η .

According to the eikonal eqn. (5), the normal velocity at point Q is defined as

$$v_Q = v_0 - D\kappa_Q. \quad (11)$$

As mentioned above, in media of low excitability the wavefront is rather thin, and points q and Q are so close to each

other that $v_Q \approx v_q$. Therefore, we can rewrite eqn. (11):

$$v_q \approx v_0 - D\kappa_Q, \quad (12)$$

yielding

$$\eta = \frac{v_0 - v_q}{v_0}. \quad (13)$$

The value of v_q is proportional to the measured diameter of the core according to

$$v_q = \frac{\pi d}{T} = \frac{\pi d v_0}{\lambda}. \quad (14)$$

Thus we obtain the following equation

$$\eta = 1 - \frac{\pi d}{\lambda}, \quad (15)$$

which in turn allows one to calculate η from the experimentally determined kinematical parameters d and λ at different light intensities. The values of the dimensionless curvature η as a function of the illumination intensity I calculated in this way are shown in Fig. 5. The tendency is quite convincing: the larger the intensity, the smaller the curvature.

Finally, by knowing the experimental values of η and v_0 , we can calculate the theoretically expected value of the rotation period as follows:

$$T = \frac{2\pi}{\omega} = \frac{2\pi D}{\eta \varphi(\eta) v_0^2}, \quad (16)$$

where D is a free parameter. The theoretically predicted values of T are compared in Fig. 6(a) with the experimental data measured at different light intensities. The best agreement is reached when using $D = 1.6 \times 10^{-5} \text{ cm}^2 \text{ s}^{-1}$, which is consistent with the value for the BZ reaction in solution, $2.0 \times 10^{-5} \text{ cm}^2 \text{ s}^{-1}$ used by other authors.²⁴⁻³⁰

Another important characteristic parameter of the spiral wave propagation is a universal rescaling number M .²⁵ Its value, which is often referred to as the dimensionless spiral diffusion number,²⁶⁻²⁹ can be calculated by the following equation

$$M = \frac{\lambda^2}{TD} = \frac{v_0^2 T}{D}. \quad (17)$$

According to eqn. (17), the experimental value of M can be directly calculated from the measured rotation period and propagation velocity. The calculated values of M (multiplied by D) as a function of light intensity I are shown with solid circles in Fig. 6(b).

According to the kinematical theory, we can estimate the value of M by knowing the value of η only. Substituting eqn. (10) into eqn. (17) gives

$$M = \frac{2\pi}{\eta \varphi(\eta)}. \quad (18)$$

In Fig. 6(b) the estimated values (multiplied by D) are shown with open circles. There is an excellent agreement between the predicted and experimentally determined values.

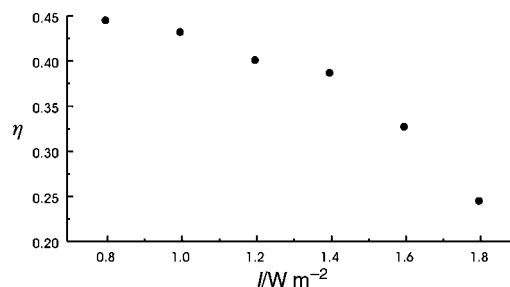


Fig. 5 Dimensionless curvature, η , as a function of the light intensity.

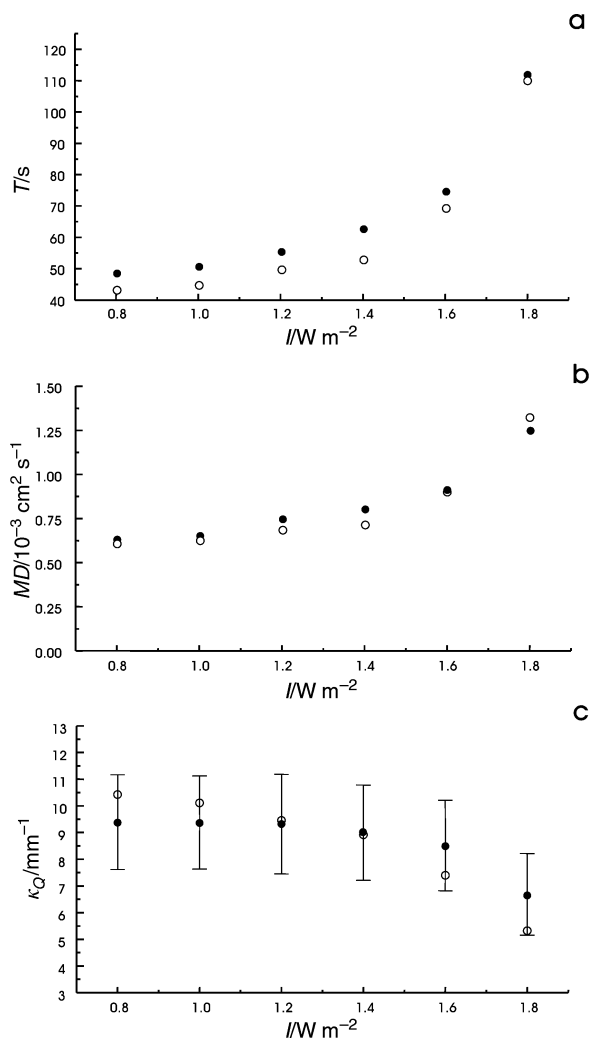


Fig. 6 Comparison of experimental data (solid circles) with the theoretical predictions (open circles) (a) rotation period, T , (b) dimensionless spiral diffusion number, M (multiplied by D), and (c) curvature, κ_Q .

Based on eqn. (9), we can now make an estimate of the curvature at point Q by using the experimentally determined values of η (see Fig. 5) and v_0 . In Fig. 6(c), the predicted values of κ_Q are shown with open circles, while the average of the experimentally determined values are shown with solid circles. This average has been obtained from more than 100 contour lines of the rigidly rotating spiral wave.

The experimental error (shown by the bars) is quite large for the following reasons. In order to determine the curvature, one has to compute the second spatial derivative of the front coordinates x , y with respect to the arc length s of the contour line determined from an experimentally observed image. This is, however, a difficult task because of the high level of the pixel noise. (Note that only a relatively small section ($\sim 20 \times 20$ pixels) of the whole image area of 512×512 pixels is considered to determine the curvature.) Still the agreement between the predicted and experimentally obtained curvature values is fairly good.

Discussion

The experimental results show that in the light sensitive BZ medium a transition from meandering to rigidly rotating spiral waves can be induced by increasing the illumination intensity. Moreover, the core size of rigidly rotating spirals significantly increases, as the light intensity is further increased. Finally, when the light intensity reaches a sufficient-

ly high value, one can observe the complete disappearance of spiral waves from the medium. In this regime, the excitability of the medium is reduced to a critical value which corresponds to the existence boundary of spiral waves.²⁵ In the vicinity of this boundary, both the dimensionless curvature, η , and the curvature, κ_Q , decrease to zero, while the diameter of the spiral core, d , the rotation period, T , and the dimensionless spiral diffusion number, M , grow to infinity.

The experimentally determined values of T , M and κ_Q are in good agreement with the predictions based on the kinematical theory of spiral waves, as shown in Fig. 6. The finding that the three functional dependences are well represented by the theory with only one free parameter (the diffusion coefficient D), underline the validity of this approach. The experimental data also show that in the vicinity of the existence boundary the propagation velocity, v_0 , varies only within a narrow range ($\sim 5\%$) around an average value. This strengthens the key assumption of the kinematical theory that in this case the main physical reason for the unrestricted growth of the rotation period, T , is the decrease in the curvature, κ_Q .

It was demonstrated earlier that the dimensionless spiral diffusion number, M , remains more or less constant even under rather strong variations in the chemical composition of the excitable media.^{26–29} However, in weakly excitable media, like that studied in this work, the value of M is not constant, but rather increases to infinity as the system approaches the vicinity of the spiral existence boundary. According to eqn. (18), the value of M depends on the dimensionless curvature η only, and for small η the value of M can be infinitely large. The limiting case $\eta = 0$ corresponds to the existence boundary of a spiral wave. Numerical simulations with the Oregonator model²⁵ also show the pronounced growth of M near to this boundary. Similar results have been observed during the aging of the BZ solution in a closed reactor, where the value M grows because the aging medium becomes less and less excitable in the course of time.³⁰

In the presented experiments the lowering of the excitability was achieved by a well controlled increase in the light intensity, which in turn allowed us to establish several important relationships between different kinematical characteristics of these waves. The agreement with the predictions of the kinematical theory proves that these relationships should be also valid for media of low excitability of different origin.

Acknowledgement

O.K. thanks the Deutscher Akademische Austauschdienst (DAAD) and the Postgraduate Education and Research Program in Chemistry funded by the Royal Thai Government for financial support. This work has been also supported by the Hungarian Research Grants OTKA T025375 and FKFP 0455/1997 and the European Science Foundation REACTOR.

References

- 1 J. M. Davidenko, A. V. Pertsov, R. Salomonsz, W. Baxter and J. Jalife, *Nature (London)*, 1992, **355**, 349.
- 2 S. Jakubith, H. H. Rotermund, W. Engel, A. von Oertzen and G. Ertl, *Phys. Rev. Lett.*, 1990, **65**, 3013.
- 3 A. N. Zaikin and A. M. Zhabotinsky, *Nature*, 1970, **225**, 535.
- 4 A. T. Winfree, *Science*, 1972, **175**, 634.
- 5 Th. Plesser, S. C. Müller and B. Hess, *J. Phys. Chem.*, 1990, **94**, 7501.
- 6 V. Gáspár, G. Bazsa and M. T. Beck, *Z. Phys. Chem. (Leipzig)*, 1983, **264**, 43.
- 7 L. Kuhnert, *Naturwissenschaften*, 1986, **73**, 96.
- 8 K. I. Agladze, V. A. Davydov and A. S. Mikhailov, *JETP Lett.*, 1987, **45**, 767.
- 9 O. Steinbock, V. S. Zykov and S. C. Müller, *Nature*, 1993, **366**, 322.
- 10 M. Braune and H. Engel, *Chem. Phys. Lett.*, 1993, **211**, 534.
- 11 S. Grill, V. S. Zykov and S. C. Müller, *Phys. Rev. Lett.*, 1995, **75**, 3368.

- 12 D. M. Goldschmidt, V. S. Zykov and S. C. Müller, *Phys. Rev. Lett.*, 1998, **80**, 5220.
- 13 O. Kheowan, V. S. Zykov, O. Rangsiman and S. C. Müller, *Phys. Rev. Lett.*, 2001, **86**, 2170.
- 14 W. K. Burton, N. Cabrera and F. C. Frank, *Philos. Trans. R. Soc. London, Ser. A*, 1951, **243**, 299.
- 15 V. S. Zykov, *Simulation of Wave Processes in Excitable Media*, Manchester University Press, Manchester, 1987, p. 113.
- 16 J. J. Tyson and J. P. Keener, *Physica D*, 1988, **32**, 327.
- 17 T. Yamaguchi, L. Kuhnert, Zs. Nagy-Ungvárai, S. C. Müller and B. Hess *et al.*, *J. Phys. Chem.*, 1991, **95**, 5831.
- 18 S. Grill, V. S. Zykov and S. C. Müller, *J. Phys. Chem.*, 1996, **100**, 19082.
- 19 G. S. Skinner and H. L. Swinney, *Physica D*, 1991, **48**, 1.
- 20 N. Wiener and A. Rosenblueth, *Arch. Inst. Cardiol. Mex.*, 1946, **16**, 205.
- 21 A. Lázár, H.-D. Försterling, H. Farkas, P. Simon, A. Volford and Z. Noszticzius, *Chaos*, 1997, **7**, 731.
- 22 A. Volford, P. Simon, H. Farkas and Z. Noszticzius, *Physica A*, 1999, **274**, 30.
- 23 P. K. Brazhnik, V. A. Davydov and A. S. Mikhailov, *Sov. Phys.—Theor. Math. Phys.*, 1988, **74**, 300.
- 24 P. Foerster, S. C. Müller and B. Hess, *Proc. Natl. Acad. Sci. USA*, 1989, **86**, 6831.
- 25 W. Jahnke and A. T. Winfree, *Int. J. Bifur. Chaos*, 1991, **1**, 463.
- 26 A. L. Belmonte and J.-M. Flesselles, *Phys. Rev. Lett.*, 1996, **77**, 1174.
- 27 A. L. Belmonte, Q. Ouyang and J.-M. Flesselles, *J. Phys. II France*, 1997, **7**, 1425.
- 28 J.-M. Flesselles, A. Belmonte and V. Gáspár, *J. Chem. Soc., Faraday Trans.*, 1998, **94**, 851.
- 29 A. F. Taylor, V. Gáspár, B. R. Johnson and S. K. Scott, *Phys. Chem. Chem. Phys.*, 1991, **1**, 4595.
- 30 Zs. Nagy-Ungvárai and S. C. Müller, *Int. J. Bifur. Chaos*, 1994, **4**, 1257.